To appear in:
International Journal of Nano Dimension (Int. J. Nano Dimens.)

Online ISSN: 2228-5059 Print ISSN: 2008-8868

Dates:
Received: 03 August 2025
Revised: 01 September 2025
Accepted: 03 September 2025

DOI: https://doi.org/10.57647/ijnd-2026-1702-04

Research Paper

Oriented external electric field effect on the adsorption of vanadocene dichloride (VDC) anticancer drug on C@Al_{12} cluster

Reza Ghiasi [1, *], Alireza Valizadeh [2], Aram Afkhami [3]

[1] *Department of Chemistry, ET.C., Islamic Azad University, Tehran, Iran*

[2] *Department of Medical Nanotechnology, School of Advanced Technologies in Medicine, University of Medical Sciences, Tehran, Iran*

[3] *Department of Research and Development, DNA Chemical Co., Tehran, Iran*

*E-mail: reza.ghiasi@iau.ac.ir, rezaghiasi1353@yahoo.com

ORCID: 0000-0002-1200-6376

Abstract

This work examined the oriented external electric field (OEEF) along x, y, and z-axes in the interaction between vanadocene dichloride (VDC) anticancer drug and C@Al_{12} cluster. OEEF effect on the electronic energy and interaction energy values was studied. These results indicated weaker adsorption in VDC…C@Al_{12} complex in the presence of OEEF along the z-axis than x, and y-axes. Variations of polarity and frontier orbital energy values of the molecule with strength of OEEF were reported. Greater polarity was found with higher OEEF strength. The most contribution in the SOMO and LUMO of the VDC…C@Al_{12} complex were belonged to C@Al_{12} and VDC moieties, respectively. Also, dependencies of reactivity parameters on OEEF strength were provided. Cl···Al interactions were illustrated with **electron localization function (**ELF**) and** charge displacement curves (CDC) **results.**

Keywords: Charge displacement curves (CDC); C@Al_{12} (E=C, Si) cluster; **Electron localization function (**ELF**);** Oriented external electric field (OEEF); Vanadocene dichloride (VDC).

Introduction

One of the organometallic anticancer drugs is vanadocene dichloride ([Cp_2VCl_2], VDC) [1, 2]. Preclinical analyses with animal and human cell lines have been investigated about this drug. VDC has been significant results in comparison to other [3, 4]. In a research, hydrolysis Chemistry, equilibria, aqueous kinetics, and mechanistic consequences of the VDC have been reported [5]. Significant action of vanadocene derivatives causes to identification of action mechanism of these complexes is not completely recognized. Biotransformation in the cellular surroundings rests indefinable and, so, it needs to be discovered if and in what way VDC or its derivatives could coordinate to DNA inside the nucleus next administration. The hypothesis that V compounds influence the target cells in the similar system as they are directed is a generalization [6].

Structures and properties of pure and mixed aluminum clusters have been demonstrated [7-11]. Between numerous clusters, superatoms are a category of distinct clusters simulating the atoms chemistry [12, 13]. For instance, Al_{12} performs as a superatom, and addition of C atom changes its electronic structure and structure and characteristic. Various computation studies have been reported about the geometry, optical, and spectroscopic properties of this cluster. For example, carbon dioxide adsorption on $Al_{12}X$ (X = transition metals or main group metals) clusters has been reported [14]. In another article, @Al_{12} (X = Al^-, P^+, C, Si) molecules with O_2 molecule has been illustrated [15]. Also, several biological studies have been reported about of these molecules category. In a DFT study, interactions of DNA and $Al_{12}X$ (X = P, N, C, and Al) clusters has been explored [16]. In other research, interaction of DNA nucleobases/base pairs and $Al_{12}Be$ molecule has been illustrated [17].

Customary drug delivery frequently suffers from non-specific distribution, poor bioavailability, frequent dosing requirements and increased side effects. Nanomedicine statements have been these problems by permitting precise, sustained, and targeted drug delivery. Drug delivery with nano-structures has been exemplified in numerous systems using computational approaches [18-31]. Effective different factors in drug delivery have been illustrated. For instance, solvent effect in these systems has been investigated [32, 33]. In a computational research interactions of the C_{20} and $M^+@C_{20}$ (M= Li, Na, K) clusters with VDC drug have been reported [34]. In another paper, the interactions between VDC drug and E@Al_{12} (E=C, Si) nano-cages were explained [35].

Oriented external electric field (OEEF) impacts many properties of molecules. For instance, OEEF influences electronic, geometric structure [36], and the chemical reactivity [37-42] of molecules. Also, electric fields may help as a trigger for drug release from drug delivery systems [43, 44]. The experienced OEEF of molecules depends on to the uses and differs from may microvolts per meter ($\mu V.m^{-1}$) to mega volt per meter ($MV.m^{-1}$). 100 ms pulse lengths are considered in biology. On the other hand, OEEFF strength of

1000 V.cm^{-1} was used to deliver low MW medicines into mammalian cells, whereas, longer pulses and lower fields were employed for the delivery of genes. It is well known biological systems are capable to contain a strong field in the ~10^8 to ~10^{10} V m^{-1} range [45, 46].

According to our researches, OEEF effect on the interaction between the anticancer active molecules Cp_2VCl_2 and C@Al_{12} cluster has been not reported. Therefore, illustration of OEEF effect on the interaction between the VDC and C@Al_{12} cluster was attractive for us using DFT calculations.

Computational methods

Gaussian 09 software, was used for optimization and vibrational analysis of the studied systems [47]. The Def2-TZVPPD [48-50] and 6-311G(d,p) [51-54] basis sets were choose for transition metal atom and main group atoms, respectively. Spin multiplicity and charge of VDC…C@Al_{12} complex were considered as doublet and neutral states, respectively. Computations were considered with the BP86 functional [55, 56]. This functional is one of the generalized gradient approximation (GGA) functional. Various investigations have been revealed BP86 as valuable functional for exploring the electronic structure, bonding, and properties of an extensive variety of vanadium compounds [57-59]. Vibrational analysis agreed the minimum character of the optimized geometries.

The interaction energy (ΔE_{int}) values of between VDC drug and C@Al_{12} cluster are provided as:

$$\Delta E_{int} = E(VDC \dots C@Al_{12}) - E(VDC) - E(C@Al_{12}); equation\ 1$$

Corrected adsorption energy is computed as:

$$\Delta E_{int}^{corr} = \Delta E_{int} + E(BSSE); equation\ 2$$

Where E(BSSE) shows, basis set superposition error (BSSE) corrected for interaction energy [60, 61].

The electron localization function (ELF) is a useful technique to graphically explain the covalent interaction. The idea of ELF is defined as [62-64]:

$$ELF = \left[1 + \frac{\frac{1}{2}\sum_i |\nabla\psi_i|^2 - \frac{1}{8}\frac{|\nabla\rho|^2}{\rho}}{\frac{3}{10}(3\pi^2)^{\frac{2}{3}}\rho^{\frac{5}{3}}}\right]^{-1}; equation\ 3$$

where the ρ; $\nabla\rho$ and $|\psi_i|^2$ are the electron density, its gradient, and the kinetic energy density, respectively. The rang of ELF is within 0–1. A great ELF value reveals that electrons are importantly localized; representing that there will be a covalent bond.

Electron localization function (ELF) [35, 62-65] and charge displacement curves (CDC) were provided using Multiwfn 3.8 software package [66, 67].

Results and discussion

1. Energetic aspect

Optimized geometry and coordinated axes of VDC…C@Al_{12} complex are shown in Figure 1. Calculated energy data of the VDC…C@Al_{12} molecule are gathered in Table 1 in the absence and presence of OEEF along x, y, and z-axes. It can be provided, higher energy values in the presence of OEEF along x, y, and z-axis than the absence of OEEF. These energy data rise with increasing of OEEF strength along the x-axis from 0.001 to 0.003 a.u (1 a.u= 51.4 V/Å = 51.4 $\times 10^{10}$ V/m). Therefore, the energetic stability of the complex decreases in this range. But, energy data decrease with enhancing of OEEF strength along the x-axis from 0.003 to 0.005 (a.u). Hence, the energetic stability of the complex rises in this range. Computed energy values decrease with increasing of OEEF strength along y, z-axes from 0.001 to 0.005 (a.u). As a result, energetic stability of the complex enhances in this series. Differences of energy values in the presence and absence of OEEF (ΔE_1) are listed in Table 1. It can be provided quadratic equations between $\Delta E_{1,y}$ and $\Delta E_{1,z}$ with OEEF strength (E_q) values:

$$\Delta E_{1,y} = -73.04\ E_y^2 - 0.73\ E_y + 0.016; \qquad R^2 = 0.9999$$

$$\Delta E_{1,z} = -70.539\ E_z^2 - 2.58\ E_z - 0.007; \qquad R^2 = 1.00$$

On the other hand, greater energy values are found in the presence of OEEF along the x-axis than y, and z-axes for the complex. It can be deduced, the larger energetic stability of the complex along y, z-axes concerning the x-axis. Differences of energy values along the x, and y-axes, and z-axis (ΔE_2) are listed in Table 1. It can provide a good linear correlation between $\Delta E_{2,x}$ with OEEF strength (E_x) values:

$$\Delta E_{2,x} = 28.20\ E_x + 1.386; \qquad R^2 = 0.986$$

Computed $\Delta E_{2,y}$ values show similar energetic stability for the complex in the presence of OEEF along y, z-axes.

2. Interaction energy values

Calculated interaction energy (ΔE_{int}) values of between VDC drug and C@Al_{12} cluster are collected in Table 2. These values expose weaker adsorption in VDC…C@Al_{12} in the presence of OEEF along the z-axis than x, and y-axes. Therefore, relaxation of the drug occurs easier in the presence of OEEF along the z-axis in comparison to x, and y-axes.

3. Polarity

The dipole moment values of the considered molecules are summarized in Table 2. Figure 2 indicated the direction of the dipole moment vector in the optimized VDC…C@Al_{12} complex.

It can be understood, that the polarity of the complex decreases in the presence of OEEF along the x-axis than absence of OEEF. Dipole moment values fall with the enhancement of OEEF strength from 0.001 to 0.003 (a.u). However, the polarity of the complex enhances with increasing of OEEF strength than 0.003 (a.u).

Polarity of the complex has been increased in the presence of OEEF along y, and z-axes. Larger polarity is observed with increasing of strength of OEEF. On the other hand, the polarity of the complex increases along coordination axes as $y < z < x$.

4. Structural parameters

It is essential to remark that the structures might experience some variations in permitting the fragments to optimize under the applied **fi**eld. So, we have attained the optimized structures of VDC…C@Al_{12} complex at different field. Cl…Al distances in the optimized structures of VDC…C@Al_{12} complex are summarized in Table 3 in the absence and presence of OEEF. We do not detect any considerable changes in the bond length and bond angles upon OEEF. When field strength along the z-axis is applied, we detected smaller Cl-V-Cl bond angles compared to x, and y-axes (by ∼1.0°).

5. Molecular orbital analysis

Figure 3 shows plots of SOMO and LUMO of the VDC…C@Al_{12} complex in the absence of OEEF. Similar plots have been provided in the presence of OEEF. It can be observed that C@Al_{12} and VDC include the most contribution in the SOMO and LUMO, respectively.

The frontier orbitals energy and the subsequent SOMO–LUMO gaps values of VDC…C@Al_{12} complex are recorded in Table 4 in the absence and presence of OEEF along x, y, and z-axes.

SOMO energy

It can be reasoned; that E(SOMO) values are greater in the presence of OEEF than absence of OEEF along the x-axis. These values rise with the increase of larger OEEF strength along the x-axis. So, smaller SOMO stability is found in the presence of stronger OEEF strength along the x-axis.

There is a worthy linear correlation between SOMO energy values and OEEF strength:

$$E(SOMO) = 1.213\ E_x - 4.45; \qquad R^2 = 0.9989;\ E_x > 0$$

On the other hand, SOMO energy values are decreased in the presence of OEEF along y, and z-axes than absence of OEEF. E(SOMO) values reduce with increasing OEEF strength along y, z-axes. Hence, SOMO stability is enhanced in the presence of stronger OEEF strength along y, z-axes.

Again, good relationships are provided between SOMO energy values and OEEF strength:

$$E(SOMO) = -0.123\ E_y - 4.4192; \qquad R^2 = 0.9662;\ E_y > 0$$

$$E(SOMO) = -0.149\ E_z - 4.409; \qquad R^2 = 0.9839;\ E_z > 0$$

The smallest E(SOMO) values are established in the presence of OEEF along the y-axis. Accordingly, more SOMO stability is concluded in the presence of OEEF along the y-axis than x, and z-axes.

LUMO energy

Computed LUMO energy values reveal bigger E(LUMO) values in the presence of OEEF along x, y, and z-axes. Hence, a smaller stability of LUMO is observed in the presence of OEEF.

E(LUMO) values increase with the growth of OEEF strength along the x-axis from 0.001 to 0.003 (a.u). But, LUMO energy values reduce with growing of larger OEEF strength than 0.003 (a.u).

On the other hand, LUMO energy values are decreased in the presence of OEEF along y, and z-axes rather than in the absence of OEEF. E(LUMO) values reduce with growing OEEF strength along y, z-axes. Consequently, greater LUMO stability is deduced in the presence of stronger OEEF strength along y, z-axes.

Worthy relationships are provided between LUMO energy values and OEEF strength along y, z-axes:

$$E(LUMO) = -0.91\ E_y - 3.4017; \qquad R^2 = 0.9707$$

$$E(LUMO) = -0.114\ E_z - 3.416; \qquad R^2 = 0.9992$$

The smallest E(LUMO) value is found in the presence of OEEF along the z-axis. Thus, greater LUMO stability is inferred in the presence of OEEF along the z-axis than x, and y-axes.

6. Variation of the Reactivity Parameters

Now we examined the effect of such an OEEF on the global reactivity descriptors of the VDC…C@Al_{12} complex. Hardness, chemical potential, and electrophilicity values of VDC…C@Al_{12} complex are noted in Table 4 in the absence and presence of OEEF along the x-axis.

SOMO-LUMO gap

Larger SOMO-LUMO gap values are provided in the presence of OEEF than in the absence of OEEF. These values decrease with enhancing of OEEF strength along the x-axis. A good linear correlation is found between SOMO-LUMO gap values and OEEF strength:

$$Gap = -1.317\ E_x + 1.14; \qquad R^2 = 0.9818;\ E_X>0$$

It can be observed, that their minor variations in corresponding values with OEEF values along y, and z-axes.

Chemical potential

The chemical potential of evaluates the escaping tendency of the electrons from a molecule. Computed chemical potential values show larger μ values in the presence OEEF than the absence of OEEF. These values enhance with enhancing OEEF strength along the x-axis. A good linear correlation is deduced between chemical potential values and OEEF strength:

$$\mu = 0.554\ E_x - 3.878; \qquad R^2 = 0.9871;\ E_X>0$$

On the other hand, corresponding values reduce with enhancing of OEEF strength along the y, z-axes.

Smaller chemical potential data are established in the presence of OEEF along the z-axis than x, y-axes.

Electrophilicity

Calculated electrophilicity values display smaller ω values in the presence of OEEF than absence of OEEF. These data increase with growing of OEEF strength along the x-axis. A respectable linear correlation between ω values and OEEF strength can be accessible:

$$\omega = 17.78\ E_X + 12.72; \qquad R^2 = 0.9320;\ E_X>0$$

There are insignificant variations in corresponding values with OEEF values along y, and z-axes.

The reactivity parameters variations obviously specify a strong interaction of the molecule with the applied field. It is hence concluded that any environment creating an electric field inform a great effect on the reactivity of the complex.

The low μ value and large ω value of electrophilicity index for a molecule approval its electrophilic behavior. In the similar manner, the large μvalue of chemical and small ω value of electrophilicity index incline its nucleophilic activities.

7. ELF

The ELF of the adsorption of VDC on C@Al_{12} is presented in Figure 4 (a). The red regions specify the region with considerable electron density while the regions with green designate the region with moderate electron densities.

It displays that the ELF in the areas between the Cl atoms and Al atoms is about 0.14 and 0.17 at bond critical points of Al…Cl and Al…Cl, respectively**.** These results further confirm the weak interaction of Cl atom of VDC and the Al atom of the C@Al_{12} cluster. Therefore, easier relaxation of the drug is occurred in the VDC**…**C@Al_{12} complex.

8. Charge displacement curve (CDC)

A charge displacement curve (CDC) is a significance method considered to imagine and explore the flow of electron density, mainly during chemical bonding or charge transfer at interfaces. CDCs of the considered molecules are shown in Figure 4 (b). In this figure, the green and blue areas characterize the sections wherever electron density is enhanced and reduced after the interaction is occurred, respectively.

Conclusion

Computational assessment of OEEF on the adsorption of VDC anticancer drug on the C@Al_{12} cluster specified greater energy data in the presence of OEEF along the x-axis than y, z-axes for the complex. Interaction energy values revealed easier relaxation of the drug in the presence of OEEF along the z-axis in comparison to x, and y-axes. The polarity of the complex increases in the presence of OEEF along y, and z-axes. Larger polarity was observed with increasing the strength of OEEF. On the other hand, the polarity of the complex increased along coordination axes as $y < z < x$. SOMO-LUMO gap values reduced with enhancing OEEF strength along the x-axis. Lower chemical potential values were found with increasing OEEF strength along the y, z-axes. Computed ELF vales at bond critical points of Al…Cl confirmed weak interaction between the Cl atoms and Al atoms. In the future of our investigations, we intent to exploring of adsorption of VDC on the E@Al_{12} (E= Si, Ge, Sn, Pb) clusters.

Author's contribution:

R. Ghiasi: Supervision, Conceptualization, Data curation, Investigation, Formal analysis

A. Valizadeh: Methodology, Data curation, Writing, Review and Editing

A. Afkhami: Methodology, Data curation, Writing, Review and Editing

Funding: No funds or grants were received.

Data availability: Data will be made available on request.

Ethics declarations

Ethical Approval

Not applicable.

Compliance with ethical standards

Conflict of interest: The authors declare that they have no conflict of interest.

Consent to participate: All the co-authors consent to participate.

Consent to publish: All the co-authors consent to publish

References

1. Köpf-Maier P., Krahl D., (1983), Tumor inhibition by metallocenes: Ultrastructural localization of titanium and vanadium in treated tumor cells by electron energy loss spectroscopy. *Chem.-Biol. Interact.* . 44: 317−328,doi 10.1016/0009-2797(83)90059-5.
2. Köpf-Maier P., Köpf H., (1987), Non-platinum group metal antitumor agents. History, current status, and perspectives. *Chem. Rev.* 87: 1137−1152,doi 10.1007/s002800050838.
3. Lümmen G., Sperling H., Luboldt H., Otto T., Rübben H., (1998), Phase II trial of titanocene dichloride in advanced renal-cell carcinoma. *Cancer Chemother. Pharmacol.* 42: 415−417,doi 10.1007/s002800050838.
4. Kröger N., Kleeberg U.R., Mross K., Edler L., Hossfeld D.K., (2000), Phase II clinical trial of titanocene dichloride in patients with metastatic breast cancer. *Onkologie* 23: 60−62,doi 10.1159/000027075.
5. Toney J.H., Marks T.J., (1985), Hydrolysis Chemistry of the Metallocene Dichlorides M(h^5-$C_5H_5)_2C1_2$, M = Ti, V, Zr. Aqueous Kinetics, Equilibria, and Mechanistic Implications for a New Class of Antitumor Agents. *J. Am. Chem. Soc.* 107: 947-953,doi 10.1021/ja00290a033.
6. Yoshikawa Y., Sakurai H., Crans D.C., Micera G., Garribba E., (2014), Structural and redox requirements for the action of anti-diabetic vanadium compounds. *Dalton Trans.* 43: 6965–6972,doi 10.1039/C3DT52895B.
7. Page A.J., Saha S., Li H.B., Irle S., Morokuma K., (2015), Quantum Chemical Simulation of Carbon Nanotube Nucleation on Al_2O_3 Catalysts via CH_4 Chemical Vapor Deposition. *J. Am. Chem. Soc.* 137: 9281-9288,doi 10.1021/jacs.5b02952.
8. Deshpande M.D., Kanhere D.G., (2003), Ab initio absorption spectra of Al_n (n =2–13) clusters. *Phys. Rev. B.* 68: 035428,doi 10.1103/PhysRevB.68.035428.
9. Aguado A., López J.M., (2009), Structures and stabilities of

Al^{+n}, Al_n,, and Al^{-n} (n=13-34 clusters. *J. Chem. Phys.* 130: 064704,doi 10.1063/1.3075834.
10. Pettersson L.G.M., C. W. Bauschlicher J., Halicioglu T., (1987), Small Al clusters. II. Structure and binding in Al_n (n=2–6, 13). *J. Chem. Phys.* 87: 2205-2213,doi 10.1063/1.453147.
11. Cox D.M., Trevor D.J., Whetten R.L., Rohlfing E.A., Kaldor A., (1986), Aluminum clusters: Magnetic properties. *J. Chem. Phys.* 84: 4651-4656,doi 10.1063/1.449991.
12. Luo Z., W. C.A., (2014), Jr. Special and general superatoms. *Acc. Chem. Res.* 47: 2931−2940,doi 10.1021/ar5001583.
13. Reber A.C., Khanna S.N., (2017), Superatoms: Electronic and

geometric effects on reactivity. *Acc. Chem. Res.* 50: 255−263,doi 10.1021/acs.accounts.6b00464.
14. Zhao J.-Y., Zhao F.-Q., Xu S.-Y., Ju X.-H., (2014), Theoretical study of the geometries and decomposition energies of CO_2 on $Al_{12}X$: Doping effect of $Al_{12}X$. *Journal of Molecular Graphics and Modelling.* 45: 9–17,doi 10.1016/j.jmgm.2013.11.002.
15. Lu Q.L., Chen L.L., Wan J.G., G H.W., (2010), First Principles Studies on the Interaction of O_2 with $X@Al_{12}$ ($X = Al^-, P^+$, C, Si) Clusters. *Journal of Computational Chemistry.* 31: 2804-2809,doi
16. P.Jin, Chen Y., Zhang S.B., Chen Z., (2012), Interactions between $Al_{12}X$ (X = Al, C, N and P) nanoparticles and DNA nucleobases/base pairs: implications for nanotoxicity. *J Mol Model.* 18: 559–568,doi 10.1007/s00894-011-1085-5.
17. Zhang X.-L., Zhang L., Chen J.-H., Li C.-Y., Sun W.-M., (2020), On the Interaction between Superatom $Al_{12}Be$ and DNA Nucleobases/Base Pairs: Bonding Nature and Potential Applications in O_2 Activation and CO Oxidation. *ACS Omega 2020.* 5: 15325−15334,doi 10.1021/acsomega.0c01375.
18. Ghanbari H., Cousins B.G., Seifalian A.M., (2011), A nanocage for nanomedicine: Polyhedral oligomeric silsesquioxane (POSS). *Macromol Rapid Commun.* 32: 1032–1046,doi 10.1002/marc.201100126.
19. Kazemi Z., Ghiasi R., Jamehbozorgi S., (2018), Analysis of the Interaction Between the C<inf>20</inf> Cage and cis-$PtCl_2(NH_3)_2$: A DFT Investigation of the Solvent Effect, Structures, Properties, and Topologies. *Journal of Structural Chemistry.* 59: 1044-1051,doi 10.1134/S0022476618050050.
20. Ghasemi A.S., Ashrafi F., Babanejad S.A., Elyasi A., (2019), Study of the Physicochemical Properties of Anti-Cancer Drug Gemcitabine on the Surface of Al Doped C_{60} and C_{70} Fullerenes: A DFT Computation. *J. Struc. Chemi.* 60: 13-19,doi 10.1134/S0022476619010037.
21. Mirali M., Jafariazar Z., Mirzaei M., (2021), Loading Tacrine Alzheimer's Drug at the Carbon Nanotube: DFT Approach. *LAB-IN-SILICO.* 2: 3-8,doi 10.22034/labinsilico21021003.
22. Ghiasi R., Valizadeh A., (2023), Computational Investigation of Interaction of a Cycloplatinated Thiosemicarbazone as Antitumor and Antiparasitic Agents with $B_{12}N_{12}$ Nano-Cage. *Results in Chemistry.* 5: 100768,doi 10.1016/j.rechem.2023.100768.
23. Ghiasi R., Emami R., Sofiyani M.V., (2021), Interaction between carboplatin with $B_{12}P_{12}$ and $Al_{12}P_{12}$ nano-clusters: A computational investigation *Phosphorus, Sulfur, and Silicon and the Related Elements.* 196: 751–759,doi 10.1080/10426507.2021.1920590.
24. Ghiasi R., Sofiyani M.V., Emami R., (2021), Computational investigation of interaction of titanocene dichloride anti-cancer drug with carbon nanotube in presence of external electric field. *Biointerface Research in Applied Chemistry.* 11: 12454 - 12461,doi 10.33263/BRIAC114.1245412461.
25. Shabani M., Ghiasi R., Zare K., Fazaeli R., (2020), Quantum chemical study of interaction between titanocene dichloride anticancer drug and $Al_{12}N_{12}$ nano-cluster *Russian Journal of Inorganic Chemistry.* 65: 1726–1734,doi 10.1134/S0036023620110169.
26. Maurya A., Mishra A.N., Srivastavaa J., Mishra S., Pal M., Shukla R., Siddiqui Z., Kurban M., Prasad O., Sinha L., (2025), Drug delivery potential of γ-graphyne, 6,6,12-graphyne and γ-graphdiyne for 5-Fluorouracil: insights from DFT calculations. *Composite Interfaces.* 32: 1193-1213 doi 10.1080/09276440.2025.2460350.
27. Kurban M., Muz İ., (2024), Investigating the potential use of (ZnO)60 nanoparticle as drug delivery system for chloroquine, hydroxychloroquine, favipiravir, and remdesivir. *Materials Today Communications.* 38: 108488,doi 10.1016/j.mtcomm.2024.108488.
28. Bechohra L.L., Kurban M., Medigue N.E.H., Kellou-Taïri S., (2024), Drug delivery potential of carbon and boron nitride nanotubes: A DFT-D3 analysis of curcumin binding interactions. *Diamond and Related Materials.* 149: 111626,doi 10.1016/j.diamond.2024.111626.
29. Shabavi Z.M., Shakerzadeh E., Yadav T., Tahmasebi E., Kaviani S., Anota E.C., (2024), A DFT study on the potential application of metal-encapsulated $B_{12}N_{12}$ nanocage for efficient removal of gemifloxacin in aqueous medium. *Computational and Theoretical Chemistry.* 1234: 114535,doi 10.1016/j.comptc.2024.114535.
30. Khajavian M., Kaviani S., Piyanzina I., Tayurskii D.A., Nedopekin O.V., Haseli A., (2024), Amide-functionalized g-C_3N_4 nanosheet for the adsorption of arsenite (As^{3+}): Process optimization, experimental,

and density functional theory insight. *Colloids and Surfaces A: Physicochemical and Engineering Aspects.* 690: 133803,doi 10.1016/j.colsurfa.2024.133803.
31. Shahab S., Sheikhi M., Khancheuski M., Yahyaei H., Almodarresiyeh H.A., Kaviani S., (2022), DFT, molecular docking and ADME prediction of tenofovir drug as a promising therapeutic inhibitor of SARS-CoV-2 M^{pro}. *Main Group Chemistry.* 22: 115128,doi 10.3233/MGC-220046.
32. Solgi A., Ghiasi R., Baniyaghoob S., (2023), PCM, ETS-NOCV, and CDA investigations of interactions of a Cycloplatinated Thiosemicarbazone as Antiparasitic and Antitumor Agents with C_{20} Nano-Cage. *International Journal of Nano Dimension.* 14: 219-226,doi 10.22034/ijnd.2023.1982969.2212.
33. Ghiasi R., Rahimi M., (2021), Complex formation of Titanocene Dichloride Anticancer and $Al_{12}N_{12}$ Nano-cluster: A Quantum Chemical Investigation of Solvent, Temperature and Pressure Effects. *Main Group Chemistry.* 20: 19–32,doi 10.3233/MGC-210034.
34. Ghiasi R., Nikbakht M., Pasdar H., (2024), Interactions of the Potential Antitumor Agent Vanadocene Dichloride with C_{20} and $M^{+}@C_{20}$ (M= Li, Na, K) nano-cages: A DFT investigation. *Results in Chemistry.* 9: 101659,doi 10.1016/j.rechem.2024.101659.
35. Lu T., Chen F., (2011), Meaning and Functional Form of the Electron Localization Function. *Acta Phys. -Chim. Sin.* 27: 2786-2792,doi 10.3866/PKU.WHXB20112786.
36. Neog B., Sarmah N., R.Kar, Bhattacharyya P.K., (2011), Effect of external electric field on aziridinium ion intermediate: A DFT study. *Computational and Theoretical Chemistry.* 976: 60–67,doi 10.1016/j.comptc.2011.08.002.
37. Bhattacharyya P.K., (2015), Effect of external electric field on ground and singlet excited states of phenylalanine: A theoretical study. *Computational and Theoretical Chemistry* 1057: 43–53,doi 10.1016/j.comptc.2015.01.017.
38. Zahedi E., Mozaffari M., Karimi F.-S., Nouri A., (2014), Density functional theory study of electric field effects on the isomerization of a photochromic molecular switch based on 1,2-dithienylethene. *Can. J. Chem. .* 92: 317–323 doi 10.1139/cjc-2013-0589.
39. Kramer K.H., Bernstein R.B., (1964), Sudden approximation Applied to rotational excitation of molecules by atoms I. Low angle scattering. *J. Chem. Phys.* 40: 200–203,doi 10.1063/1.1724862.
40. Brooks P.R., Jones M.E., (1966), Reactive scattering of K atoms from oriented CH_3I molecules. *J. Chem. Phys. .* 45: 3449–3450,doi 10.1063/1.1728128.
41. Shaik S., Mandal D., Ramanan R., (2016), Oriented electric fields as future smart reagents in chemistry. *Nature Chemistry.* 8: 1091-1098,doi 10.1038/nchem.2651
42. Aragonès A.C., Haworth N.L., Darwish N., Ciampi S., Bloomfield N.J., Wallace G.G., Diez-Perez I., Coote M.L., (2016), Electrostatic catalysis of a Diels-Alder reaction. *Nature* 531: 88-91,doi 10.1038/nature16989.
43. Ge J., Neofytou E., Cahill T.J., Beygui R.E., Zare R.N., (2012), Drug Release from ElectricField-Responsive Nanoparticles. *ACS Nano.* 6: 227–233,doi 10.1021/nn203430m.
44. Kolosnjaj-Tabi J., Gibot L., Fourquaux I., Golzio M., Rols M.-P., (2019), Electric field-responsive nanoparticles and electric fields: Physical, chemical, biological mechanisms and therapeutic prospects. *Advanced Drug Delivery Reviews.* 138: 56-67,doi 10.1016/j.addr.2018.10.017.
45. Bandrauk A.D., Sedik E.S., Matta C.F., (2004), Effect of absolute laser phase on reaction paths in laser-induced chemical reactions. *J. Chem. Phys.* 121: 7764−7775,doi 10.1063/1.1793931.
46. Arabi A.A., Matta C.F., (2011), Effects of external electric fields on double proton transfer kinetics in the formic acid dimer. *Phys. Chem. Chem. Phys.* 13: 13738−13748,doi 10.1039/C1CP20175A.
47. Frisch M.J., Trucks G.W., Schlegel H.B., Scuseria G.E., Robb M.A., Cheeseman J.R., Scalman G., Barone V., Mennucci B., Petersson G.A., Nakatsuji H., Caricato M., Li X., Hratchian H.P., Izmaylov A.F., Bloino J., Zheng G., Sonnenberg J.L., Hada M., Ehara M., Toyota K., Fukuda R., Hasegawa J., Ishida M., T. Nakajima, Honda Y., Kitao O., Nakai H., Vreven T., Montgomery J.A., Jr., Peralta J.E., Ogliaro F., Bearpark M., Heyd J.J., Brothers E., Kudin K.N., Staroverov V.N., Kobayashi R., J. Normand, Raghavachari K., Rendell A., Burant J.C., Iyengar S.S., J. Tomasi, Cossi M., Rega N., Millam J.M., Klene M., Knox J.E., Cross J.B., Bakken V., Adamo C., Jaramillo J., Gomperts R., Stratmann R.E., Yazyev O., Austin A.J., Cammi R., Pomelli C., Ochterski J.W., Martin R.L., Morokuma K., Zakrzewski V.G., Voth G.A., Salvador

P., Dannenberg J.J., Dapprich S., Daniels A.D., Farkas O., Foresman J.B., Ortiz J.V., Cioslowski J., Fox D.J. *Gaussian 09*, Revision A.02; Gaussian, Inc.: Wallingford CT, 2009.
48. Rappoport D., Furche F., (2010), Property-optimized Gaussian basis sets for molecular response calculations. *J. Chem. Phys.* . 133: 134105,doi 10.1063/1.3484283.
49. Pritchard B.P., Altarawy D., Didier B.t., T. D. Gibson, Windus T.L., (2019), A New Basis Set Exchange: An Open, Up-to-date Resource for the Molecular Sciences Community. *J. Chem. Inf. Model.* 59: 4814-4820,doi 10.1021/acs.jcim.9b00725.
50. Schuchardt K.L., Didier B.T., Elsethagen T., Sun L., Gurumoorthi V., Chase J., Li J., Windus T.L., (2007), Basis Set Exchange: A Community Database for Computational Sciences *J. Chem. Inf. Model.* 47: 1045-1052,doi 10.1021/ci600510j.
51. Hay P.J., (1977), Gaussian basis sets for molecular calculations - representation of 3D orbitals in transition-metal atoms. *J. Chem. Phys.* 66: 4377-4384,doi 10.1063/1.433731.
52. Krishnan R., Binkley J.S., Seeger R., Pople J.A., (1980), self consistent molecular orbital methods. XX. A basis set for correlated wave functions. *J. Chem. Phys.* 72: 650-654,doi 10.1063/1.438955.
53. McLean A.D., Chandler G.S., (1980), Contracted Gaussian-basis sets for molecular calculations. 1. 2nd row atoms, Z=11-18. *J. Chem. Phys.* 72: 5639-5648,doi 10.1063/1.438980.
54. Wachters A.J.H., (1970), Gaussian basis set for molecular wavefunctions containing third-row atoms. *J. Chem. Phys.* 52: 1033,doi 10.1063/1.1673095.
55. Perdew J.P., (1986), Density-functional approximation for the correlation energy of the inhomogeneous electron gas. *Phys. Rev. B.* 33: 8822,doi 10.1103/PhysRevB.33.8822.
56. Perdew J.P., Wang Y., (1986), Accurate and simple density functional for the electronic exchange energy: Generalized gradient approximation. *Phys. Rev. B.* 33: 8800-8802,doi • 10.1103/physrevb.33.8800.
57. Wang L.-F., Xie L., Fang H.-L., Li Y.-F., Zhang X.-B., Wang B., Zhang Y.-F., Huang X., (2014), On the structural and electronic properties of hexanuclear vanadium oxide clusters $V_6O^{-/0}$ (n = 12–15): Is V_6O_{12} cluster planar or cage-like? *Spectrochimica Acta Part A: Molecular and Biomolecular Spectroscopy.* 131: 446–454,doi 10.1016/j.saa.2014.04.094.
58. Nguyen H.T., Nguyen M.T., (2015), Decomposition pathways of formamide in the presence of vanadium and titanium monoxides. *Phys. Chem. Chem. Phys.* 17: 16927-16936,doi 10.1039/c5cp01456e.
59. Vyboishchikov S.F., Sauer J., (2000), Gas-Phase Vanadium Oxide Anions: Structure and Detachment Energies from Density Functional Calculations. *J. Phys. Chem. A.* 104: 10913-10922,doi 10.1021/jp001936x.
60. Breneman C.M., Wiberg K.B., (1990), Determining atom-centered monopoles from molecular electrostatic potentials - the need for high sampling density in formamide conformational-analysis. *J. Comp. Chem.* 11: 361-373,doi 10.1002/jcc.540110311.
61. S. Simon M.D., Dannenberg J.J., (1996), How does basis set superposition error change the potential surfaces for hydrogen bonded dimers? *J. Chem. Phys.* 105: 11024-11031,doi 10.1063/1.472902.
62. Becke A.D., Edgecombe K.E., (1990), A simple measure of electron localization in atomic and molecular systems. *J. Chem. Phys.* 92: 5397–5403,doi 10.1063/1.458517.
63. Savin A., Nesper R., Wengert S., Fssler T.F., (1997), ELF: the electron localization function,. *Angew. Chem. Int. Ed.* 36: 1808–1832,doi 10.1002/anie.199718081.
64. Silvi B., Savin A., (1994), Classification of chemical bonds based on topological analysis of electron localization function. *Nature.* 371: 683–686,doi 10.1038/371683a0.
65. Lu T., Chen Q., (2022), Independent gradient model based on Hirshfeld partition: A new ethod for visual study of interactions in chemical systems. *J. Comput. Chem.* 43: 539,doi 10.1002/jcc.26812.
66. Lu T., Chen F., (2012), Quantitative analysis of molecular surface based on improved Marching Tetrahedra algorithm. *J. Mol. Graph. Model.* 38: 314-323 doi 10.1016/j.jmgm.2012.07.004.
67. Lu T., (2024), A comprehensive electron wavefunction analysis toolbox for chemists, Multiwfn. *J. Chem. Phys.* 161: 082503,doi 10.1063/5.0216272.

Table 1. Energy values (E, a.u) of VDC…C@Al_{12} complex in absence and presence of oriented external electric field (OEEF) along x, y, z-axes. $\Delta E_{1,q}$ and $\Delta E_{2,q}$ values are relative energy respect to absence of OEEF and relative energy respect to OEEF along z-axis (kcal/mol) with the BP86 funational, Def2-TZVPPD and 6-311G(d,p) basis sets for transition metal atom and main group atoms, respectively. (for main group atoms).

Field strength*	E_x	E_y	E_z		$\Delta E_{1,x}$	$\Delta E_{1,y}$	$\Delta E_{1,z}$		$\Delta E_{2,x}$	$\Delta E_{2,y}$	$\Delta E_{2,z}$
0.000	-5199.7131	-5199.7131	-5199.7131		0.00	0.00	0.00		2.56	0.16	0.00
0.051	-5199.7095	-5199.7133	-5199.7136		2.23	-0.18	-0.33		4.37	0.18	0.00
0.103	-5199.7077	-5199.7144	-5199.7147		3.35	-0.84	-1.02		6.09	0.23	0.00
0.154	-5199.7067	-5199.7160	-5199.7164		4.01	-1.85	-2.08		7.30	0.30	0.00
0.206	-5199.7070	-5199.7182	-5199.7187		3.78	-3.23	-3.53		8.35	0.35	0.00
0.257	-5199.7083	-5199.7210	-5199.7216		3.02	-4.99	-5.33		2.56	0.16	0.00

* in V/Å.

Table 2. Adsorption energy values (ΔE_{ads}, kcal/mol) and dipole moment values (μ, Debye) of VDC…C@Al_{12} complex in absence and presence OEEF along x, y, z-axes with the BP86 funational, Def2-TZVPPD and 6-311G(d,p) basis sets for transition metal atom and main group atoms, respectively. (for main group atoms).

Field strength	$\Delta E_{ads,x}$	$\Delta E_{ads,y}$	$\Delta E_{ads,z}$		μ_x	μ_y	μ_z
0.000	**-25.95**	**-25.95**	**-25.95**		10.18	10.18	10.18
0.051	**-28.60**	-25.92	-25.56		11.67	10.45	10.65
0.103	**-29.58**	-26.82	-25.48		14.19	10.65	11.13
0.154	**-29.68**	-26.65	-25.34		16.78	11.27	11.78
0.206	**-30.46**	-26.43	-25.96		19.47	12.07	12.49
0.257	**-31.19**	-26.11	-26.02		28.80	13.01	13.40

Table 3. Al…Cl bond length (pm) and Cl-V-Cl bond angle (in degree) in the VDC…C@Al_{12} complex in absence and presence of OEEF along x, y, z-axes with the BP86 funational, Def2-TZVPPD and 6-311G(d,p) basis sets for transition metal atom and main group atoms, respectively. (for main group atoms).

	x-axis			y-axis			z-axis			∠Cl-V-Cl	
Field **strength**	Cl*...Al	Cl...Al		Cl*...Al	Cl...Al		Cl*...Al	Cl...Al		**x-axis**	**y-axis**	**z-axis**
0.000	234.6	233.8		234.6	233.8		234.6	233.8		88.0	88.0	88.0
0.051	233.4	232.3		234.1	234.4		234.5	234.1		88.2	88.1	87.4
0.103	234.1	231.4		233.4	233.6		234.0	234.4		89.5	88.3	87.3
0.154	236.1	231.9		233.4	233.6		233.5	234.6		88.4	88.3	87.3
0.206	237.2	232.0		233.4	233.6		232.8	234.1		89.6	88.2	87.1
0.257	239.7	232.7		233.4	233.7		232.3	234.1		87.9	88.2	87.0

Table 4. Frontier orbital energy, SOMO-LUMO gap, hardness (η), chemical potential (μ) and electrophilicity (ω) values (eV) of VDC…C@Al_{12} complex in absence and presence OEEF along x, y, z-axes with the BP86 funational, Def2-TZVPPD and 6-311G(d,p) basis sets for transition metal atom and main group atoms, respectively. (for main group atoms).

x-axis

Field strength	E(SOMO)	E(LUMO)	gap	η	μ	ω
0.000	-4.39	-4.00	0.39	0.20	-4.19	44.93
0.051	-4.38	-3.32	1.06	0.53	-3.85	14.02
0.103	-4.33	-3.31	1.01	0.51	-3.82	14.41
0.154	-4.27	-3.31	0.96	0.48	-3.79	14.92
0.206	-4.20	-3.33	0.87	0.43	-3.76	16.29
0.257	-4.14	-3.35	0.79	0.40	-3.74	17.66

y-axis

Field strength	E(SOMO)	E(LUMO)	gap	η	μ	ω
0.051	-4.42	-3.41	1.02	0.51	-3.92	15.10
0.103	-4.43	-3.41	1.02	0.51	-3.92	15.02
0.154	-4.44	-3.41	1.02	0.51	-3.93	15.06
0.206	-4.44	-3.42	1.02	0.51	-3.93	15.09
0.257	-4.45	-3.43	1.02	0.51	-3.94	15.15

z-axis

Field strength	E(SOMO)	E(LUMO)	gap	η	μ	ω
0.051	-4.42	-3.42	1.00	0.50	-3.92	15.42
0.103	-4.42	-3.43	1.00	0.50	-3.93	15.48
0.154	-4.43	-3.43	1.00	0.50	-3.93	15.50
0.206	-4.44	-3.44	1.00	0.50	-3.94	15.52
0.257	-4.45	-3.45	1.00	0.50	-3.95	15.52

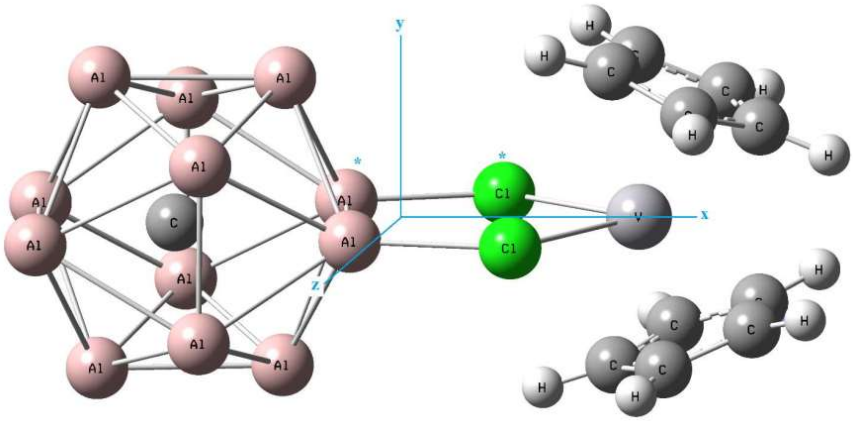

Figure 1. Geometry and directions of OEEF in the VDC…C@Al_{12} complex.

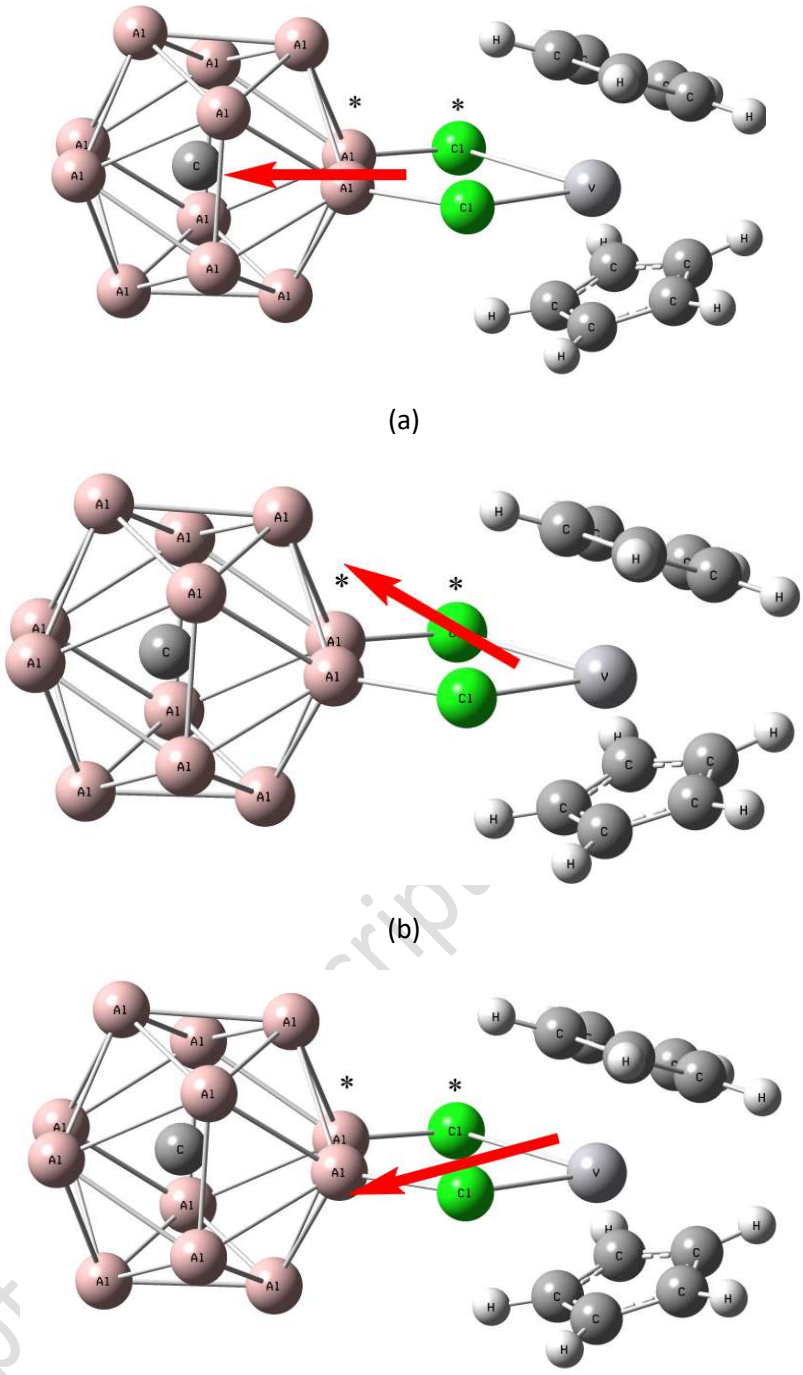

(a)

(b)

(c)

Figure 2. Direction of dipole moment vector in the VDC…C@Al_{12} complex at OEEF strength (a) from 0.001 to 0.003 a.u. along x-axis (direction of this vector is opposite in OEEF strengths larger than 0.003 a.u. (b) along y-axis, and (c) along z-axis.

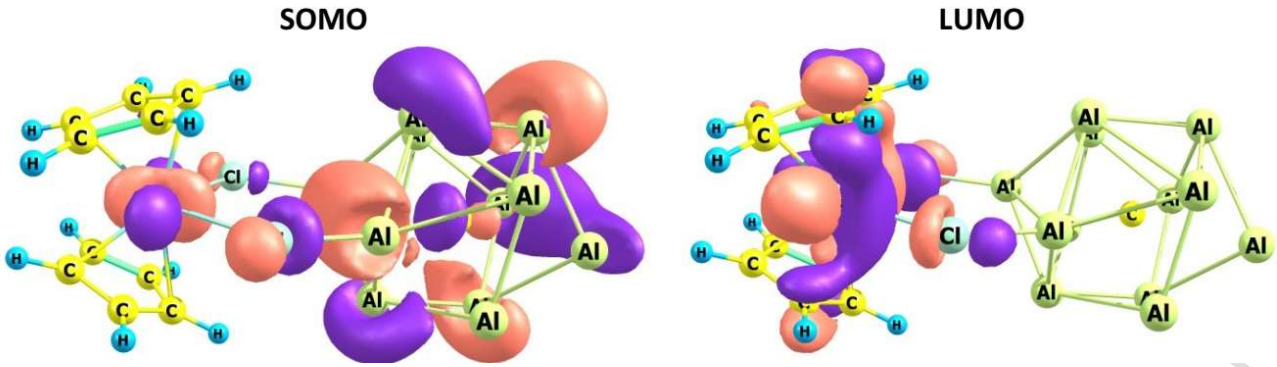

Figure 3. Plots of frontier orbitals of VDC...C@Al_{12} complex in the absence of OEEF.

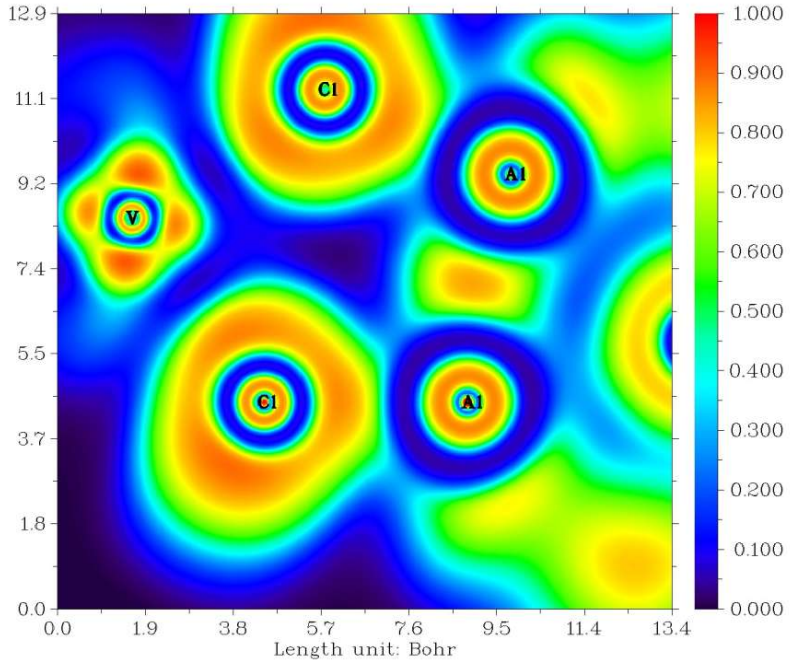

(a)

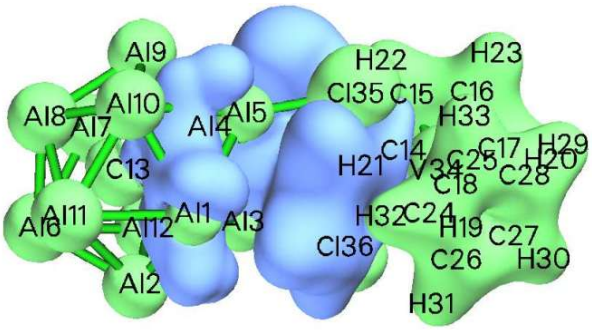

(b)

Figure 4. (a)The Color-filled maps ELF and (b) charge displacement curves (CDC) of VDC...C@Al_{12} complex in the absence of OEEF in the plane of V-Cl-Al atoms.